

# Score matching for bridges without time-reversals

Elizabeth L. Baker  
 Department of Computer Science  
 University of Copenhagen  
 Copenhagen, Denmark  
 elba@di.ku.dk

Moritz Schauer  
 Department of Mathematical Sciences  
 Chalmers University of Technology  
 and University of Gothenburg  
 smoritz@chalmers.se

Stefan Sommer  
 Department of Computer Science  
 University of Copenhagen  
 Copenhagen, Denmark  
 sommer@di.ku.dk

## Abstract

We propose a new algorithm for learning a bridged diffusion process using score-matching methods. Our method relies on reversing the dynamics of the forward process and using this to learn a score function, which, via Doob’s  $h$ -transform, gives us a bridged diffusion process; that is, a process conditioned on an endpoint. In contrast to prior methods, ours learns the score term  $\nabla_x \log p(t, x; T, y)$ , for given  $t, Y$  directly, completely avoiding the need for first learning a time reversal. We compare the performance of our algorithm with existing methods and see that it outperforms using the (learned) time-reversals to learn the score term. The code can be found at [https://github.com/libbylbaker/forward\\_bridge](https://github.com/libbylbaker/forward_bridge).

## 1 Introduction

Given a diffusion process, we consider the problem of conditioning its endpoint to take a specific value or distribution. In general it can be shown by Doob’s  $h$ -transform that a diffusion process conditioned on a point  $y$  at time  $T$  can also be written as a stochastic differential equation Equation (2), which has an extra drift term containing  $\nabla_x \log p(t, x; T, y)$ , where  $p$  is the transition density of the stochastic differential equation. The problem is, this term is general intractable. Finding alternative methods to sample from the bridge process has received considerable attention in the past [Delyon and Hu, 2006, Papaspiliopoulos and Roberts, 2012, Bladt and Sørensen, 2014, Schauer et al., 2017, Heng et al., 2022]. Diffusion processes have a multitude of applications across numerous areas, where observations need to be included, leading to bridge processes (see Papaspiliopoulos and Roberts [2012] for some examples). Recently, bridges have also been used in generative modelling via time reversals, as well as for diffusion bridges. These usually are bridges between two distributions and involve time-reversals of a linear SDE. Singhal et al. [2024] also consider using non-linear SDEs for this purpose and so look at the problem of finding time-reversed bridges of a given SDE. Within shape analysis bridges are applied, for example, to medical imaging, in order to model how the shapes of organs change in the face of disease [Arnaudon et al., 2017], or in evolutionary biology to model how shapes of organisms change over time [Baker et al., 2024].

**Contributions** We propose a new algorithm to learn bridge diffusion processes by learning the score term occurring in the conditioned process. We learn this term by combining the score matching

methods proposed in Heng et al. [2022], with adjoint diffusions [Milstein et al., 2004]. Importantly, these adjoint diffusions are not time-reversed, rather a reversal of dynamics, meaning they can be simulated directly. This differs from Heng et al. [2022], where in order to learn the score term, they first learn the time-reversed diffusion and then train a second time using the learnt time-reversed diffusions, which introduces a higher error. We compare our method with other existing methods.

## 2 Background

We are interested in conditioning an SDE to take a certain value at its end time. The conditioned process can again be written as a stochastic differential equation via Doob’s  $h$ -transform which we describe in Section 2.1. However, this SDE has an intractable term, the score term  $\nabla_x \log p(t, x; T, y)$ . In Section 2.2 we discuss the reversal (but not the time-reversal) of the SDE which, up to a correction term  $\varpi$ , has the transition density  $q(s, y; t, \cdot) = \varpi(s, y; t)^{-1} p(t, \cdot; s, y)$  when started in  $y$  at time  $s$ . In the proposed method, we will use the adjoint processes to directly learn the term  $\nabla_x \log p(t, x; T, y)$ , used for forward bridges. Score learning provides a method for learning a similar term  $\nabla_x \log p(0, x_0; t, x)$  and is discussed in Section 2.3.

### 2.1 Doob’s $h$ -transform

Consider a stochastic differential equation defined as

$$dX(t) = f(t, X(t))dt + \sigma(t, X(t))dW(t), \quad X(0) = x_0, \quad (1)$$

where  $f: [0, T] \times \mathbb{R}^d \rightarrow \mathbb{R}^d$ ,  $\sigma: [0, T] \times \mathbb{R}^d \rightarrow \mathbb{R}^{d \times m}$  and  $W(t)$  is a  $m$ -dimensional Wiener process. We assume that  $f, \sigma$  satisfies a global Lipschitz condition so that Equation (1) has a Markov solution (see Schilling and Partzsch [2014, Theorem 21.23] for details). Then  $X(t)$  has a transition density  $p(t, x; t + s, x')$ , satisfying

$$\mathbb{E}[X(t + s) \in A \mid X(t) = x] = \int_A p(t, x; t + s, x') dx'.$$

It is well known (see e.g. Särkkä and Solin [2019, Chapter 7.5]) that  $X(t)$  conditioned such that  $X(T) = y$  for a fixed  $y$ , satisfies another stochastic differential equation

$$dX^y(t) = [f(t, X^y(t)) + (\sigma \sigma^\top)(t, X^y(t)) \nabla \log p(t, X^y(t); T, y)]dt + \sigma(t, X^y(t))dW(t), \quad (2)$$

with  $X^y(0) = x_0$  and where  $\nabla$  is the gradient with respect to the argument  $X^y(t)$ . However, the transition density, or rather the score  $s(t, x) = \nabla_x \log p(t, x; T, y)$  is typically intractable.

### 2.2 Adjoint processes with reversed dynamics

Here we define the adjoint process  $\{Y(t), \mathcal{Y}(t)\}$  of the unconditioned process  $X(t)$  which receives its name from its relation to the adjoint operator of the infinitesimal generator of  $X$  seen as Markov process. Intuitively, the adjoint process has the reversed dynamics of the unconditioned process, for example, the adjoint  $Y(t)$  of a Brownian motion with drift  $\mu$ , i.e.  $W(t) + t\mu$ , is a Brownian motion with drift  $-\mu$ . In this sense, it is a reversal, but not a time-reversal as in Haussmann and Pardoux [1986]. The theory presented in this section is based on Milstein et al. [2004], Bayer and Schoenmakers [2013] and is also developed in [Van der Meulen and Schauer, 2020, Section 11]. The significance of the adjoint process is that for fixed  $T, y$ , we can use it to access  $p(t, x; T, y)$  and therefore the score  $s(t, x)$ . To compare, let  $x_0, t_0, y, T$  be fixed and  $g$  be a real-valued functional. Then

$$\mathbb{E}[g(X(t))] = \int g(x)p(0, x_0; t, x)dx, \quad \mathbb{E}[g(Y_{t,y}(T))\mathcal{Y}_{t,y}(T)] = \int g(x)p(t, x; T, y)dx. \quad (3)$$

Here,  $\mathcal{Y}$  is a weight process relating to  $\varpi$  accounting for the fact that adjoint dynamics in general are not Markovian necessitating a Feynman-Kac representation. The right hand side relation of Equation (3) will be integral in our proposed method.

For fixed  $y, t_0, T$  the adjoint process  $\{Y_{t_0,y}(t), \mathcal{Y}_{t_0,y}(t)\} \in \mathbb{R}^d \times \mathbb{R}$  is defined as follows:

$$dY = \alpha(t, Y)dt + \tilde{\sigma}(t, Y)d\tilde{W}(t), \quad Y(t_0) = y, \quad (4a)$$

$$d\mathcal{Y} = c(t, Y)\mathcal{Y}dt, \quad \mathcal{Y}(t_0) = 1. \quad (4b)$$

The functions  $\alpha, c$  are defined in terms of derivatives and second derivatives of  $f, \Sigma := \sigma\sigma^\top$  from the SDE of  $X(t)$  with  $t_0 \leq s \leq T$ :

$$\alpha^i(s, x) := \sum_{j=1}^d \frac{\partial}{\partial x^j} \Sigma^{ij}(T + t_0 - s, x) - f^i(T + t_0 - s, x), \quad (5a)$$

$$\tilde{\sigma}(s, x) := \sigma(T + t_0 - s, x), \quad (5b)$$

$$c(s, x) := \frac{1}{2} \sum_{i,j=1}^d \frac{\partial^2 \Sigma^{ij}}{\partial x^i \partial x^j}(T + t_0 - s, x) - \sum_{i=1}^d \frac{\partial f^i}{\partial x^i}(T + t_0 - s, x). \quad (5c)$$

From now on, we denote  $Y_y := Y_{0,y}$  and  $\mathcal{Y}_y := \mathcal{Y}_{0,y}$ , but the following also holds for  $t_0 \neq 0$ .

Crucially, these quantities can be computed explicitly, either by hand or using automatic differentiation, and therefore we can sample from the adjoint process using, for example, the Euler-Maruyama scheme. Moreover, following [Bayer and Schoenmakers, 2013, Theorem 3.3], we can introduce more time points. For a time grid  $\mathcal{T} = \{0 = t_0 < t_1 < \dots < t_L = T\}$ , and setting  $\hat{t}_i = T - t_{L-i}$ , it holds

$$\mathbb{E}[f(Y_y(\hat{t}_L), \dots, Y_y(\hat{t}_1))\mathcal{Y}_y(T)] = \int_{\mathbb{R}^{d \times L}} f(y_1, \dots, y_L) \prod_{i=1}^L p(t_{i-1}, y_i, t_i, y_{i+1}) dy_i, \quad y_{L+1} = y. \quad (6)$$

In particular, we can now represent the score  $s(t, x)$  as the gradient of the log density  $q(T - t, \cdot)$ , where  $q(T - t, \cdot) = p(t, x; T, y)$  is the marginal distribution of  $Y_y(T - t)$  weighted by  $\mathcal{Y}_y$ , by

$$\int_A f(x)q(\hat{t}, x)dx = \mathbb{E}[f(Y_y(\hat{t}))\mathcal{Y}_y(\hat{t}_L)], \quad \hat{t} \in [0, T]. \quad (7)$$

## 2.3 Score matching bridge sampling

In score matching bridge sampling as we consider it, the task is to learn a neural approximation  $s_\theta(t, x)$  to the score  $s(t, x) = \nabla_x \log p(t, x; T, y)$ . In our case, samples from  $Y_y(T - t)$  weighted with  $\mathcal{Y}_y(T - t)$  can be used in training, as they represent the unnormalised density  $q(T - t, \cdot) = p(t, \cdot; T, y)$ . This precisely mimics the use of samples of the noising process in generative diffusion models with  $Y_y(\hat{t}), \mathcal{Y}_y(\hat{t})$  in the role of the noising process.

To wit, vanilla score matching as introduced in Hyvärinen [2005] takes the form

$$\operatorname{argmin}_\theta \int_0^T \int q(\hat{t}, x) \sum_{i=1}^N \left[ \partial_i s_{\theta,i}(t, x) + \frac{1}{2} s_{\theta,i}(t, x)^2 \right] dx dt + \text{const.}, \quad \hat{t} = T - t. \quad (8)$$

Note in particular that knowledge of the transition density is not required. However, in general, computing the divergence term is expensive. To avoid computing the divergence term when learning  $\nabla_x \log p(0, x_0; t, x)$ , we instead use a similar loss objective to that proposed in Vincent [2011]

$$L(\theta) = \int_0^T \mathbb{E}[\|s_\theta(t, X_t) - \nabla_x \log p(0, x_0; t, X_t)\|^2] dt. \quad (9)$$

In and of itself, this optimisation problem is still intractable, however, for processes where  $p(0, x_0; t, x) = \mathcal{N}(x; \sqrt{\alpha_t}x_0, (1 - \alpha_t)\text{Id})$  for some  $\alpha$ , Ho et al. [2020] show that Equation (9) can be formulated as minimising an alternative loss function

$$L(\theta) = \mathbb{E}_{t, x_0, \xi} [\|\xi - s_\theta(t, \sqrt{\alpha_t}x_0 + \sqrt{1 - \alpha_t}\xi)\|^2]. \quad (10)$$

For processes where the transition densities are not known, Heng et al. [2022] instead suggest using the loss objective

$$L(\theta) = \sum_{l=0}^{L-1} \int_{t_l}^{t_{l+1}} \|s_\theta(t, X_t) - \nabla \log p(t_l, X_{t_l}; t, X_t)\|_{\sigma_t \sigma_t^\top}^2 dt. \quad (11)$$

Then for small time steps, the transition density  $p(t_l, X_{t_l}; t, X_t)$  can be estimated, for example, using the Euler-Maruyama scheme.

### 3 Related work

In this section, we survey the existing methods for computing bridge processes. We concentrate specifically on methods that can be applied to any diffusion process to find the forward bridge. For this reason, we deem usual score matching methods as out of scope, since the main motivation of these methods is to find a time-reversal of a specific diffusion, usually an Ornstein-Uhlenbeck.

#### 3.1 Score matching methods

Most related to our work is the method of Heng et al. [2022]. We use a similar loss function, however we take the expectation over (directly simulated) adjoint processes, enabling us to directly learn a forward in time bridge process. One key difference to the time-reversed bridge process is that the forward processes are dependent on the end point but independent of the start point, whereas the time-reversals are dependent on the start point and independent of the end point. This is because the proposed method learns the term  $\nabla_x \log p(t, x; T, y)$  with  $T, y$  fixed, whereas the method in Heng et al. [2022] learns  $\nabla_x \log p(t_0, x_0; t, x)$  with  $t_0, x_0$  fixed. Iterating over the method twice enables one to learn  $\nabla_x \log p(t, x; T, y)$ , but we show that for learning a forward in time bridge, our proposed method is advantageous in that we only need train once, thereby reducing the approximation error.

Recently, Singhal et al. [2024] consider using non-linear SDEs instead of linear ones within generative modelling, meaning the transition densities for the SDE are also unknown. However, instead of using Euler-Maruyama approximations for the transition kernels as in Heng et al. [2022], they consider other higher-order approximations. Unlike ours, their work only considers time-reversals in the context of generative modelling and not forward bridges.

#### 3.2 MCMC methods

One method of sampling from the bridge processes is to sample from a second approximate bridge, where the ratio between the true bridge and the approximate bridge is known. For an unconditional process as in Equation (1), the approximate bridges have form

$$dX(t) = f(t, X(t))dt + s(t, X(t))dt + \sigma(t, X(t))dB(t), \quad (12)$$

where different authors have considered different options for the function  $s$ . In Pedersen [1995]  $s = 0$ , that is, the samples are taken from the original unconditioned process. Delyon and Hu [2006] instead take the Brownian bridge drift term. More recently, Schauer et al. [2017] set  $s$  to be the term arising

from conditioning an auxiliary process with a known transition density. With all approximations, one can derive a ratio between the path probability of the true bridge and the bridge approximation and can therefore use Markov Chain Monte Carlo methods to sample from the true distribution.

## 4 Method

This section presents our neural-network based algorithm to find the score function  $\nabla_x \log p(t, x; T, y)$  that will be used to simulate the bridge process. In Section 4.1 we derive the main loss function for learning the score function and show it minimises the Kullback-Leibler divergence between the conditioned path and the path measure induced by the learnt conditioned process. In Section 4.2 we provide details on how we minimise the loss function. In Section 4.3 we show that we can also train for different values of  $y$ , and we can also condition on  $y$  following a distribution, instead of being a fixed point. Proofs can be found in Appendix A.1.

### 4.1 A loss function

In order to sample the bridged stochastic differential equation, we learn the score term  $\nabla_x \log p(t, x; T, y)$  for fixed  $T, y$ . Note that although similar, this is different from the term  $\nabla_x \log p(0, x_0; t, x)$  that is learnt for time-reversed processes, as in score-matching for diffusion samplers. Indeed, score-matching methods rely on the SDE  $X_t$  having  $p(0, x_0; t, x)$  as a transition density, and therefore by sampling from the process  $X_t$ , we are sampling from the distribution of the process at time  $t$ , directly leading to the transition density. This is not true for  $p(t, x; T, y)$ . Our proposal is instead to sample from the adjoint stochastic process, where we can recover the transitions  $p(t, x; T, y)$ .

Given a function  $s: [0, T] \times \mathbb{R}^d \rightarrow \mathbb{R}^d$ , we define the SDE  $X^s$  with path distribution  $\mathbb{Q}^s$  as

$$dX^s(t) = f(t, X(t))dt + (\sigma\sigma^\top)(t, X(t))s(t, X(t))dt + \sigma(t, X(t))dW(t). \quad (13)$$

In what follows, let  $K_\epsilon(x, y)$  be a function, such that  $K_\epsilon(x, y) \rightarrow \delta_0(x - y)$  as  $\epsilon \rightarrow 0$ , for  $\delta_0$  the dirac delta function. For fixed  $y, T$  with  $Y := Y_{0,y}, \mathcal{Y} := \mathcal{Y}_{0,y}$  (as defined in Equations (4a) and (4b)) and  $\hat{t} := T - t$  we introduce the functional

$$\mathcal{L}(s) = \lim_{\epsilon \rightarrow 0} \sum_{l=1}^L \int_{t_{l-1}}^{t_l} \mathbb{E}[\|s(t, Y(\hat{t})) - \nabla \log p(t, Y(\hat{t}); t_l, Y(\hat{t}))\|_{\sigma\sigma^\top}^2 \mathcal{Y}(T) K_\epsilon(Y(T), X_0)]. \quad (14)$$

By minimising this, we are minimising the Kullback-Leibler divergence between the path probability  $\mathbb{P}^y$  of  $X^y(t)$  with initial value  $x_0$  in Equation (2), and the path probability  $\mathbb{Q}^s$  of paths  $X^s$  as in Equation (13), with the same initial value  $x_0$ :

**Theorem 4.1.** Let  $X(t)$  be a diffusion process as defined in Equation (1) and suppose further that  $f, \sigma$  are  $C^2$  and that  $X$  admits  $C^2$  transition densities. Let  $X^y(t)$  be the conditioned diffusion satisfying Equation (2). Let  $\mathbb{P}^y$  be the path probability of  $X^y$  and  $\mathbb{Q}^s$  the path probability of  $X^s$  in Equation (13) for a function  $s$ . Then

$$\inf_s \text{KL}(\mathbb{P}^y \parallel \mathbb{Q}^s) = \inf_s \mathcal{L}(s),$$

where the infimum is taken over functions  $s: [0, T] \times \mathbb{R}^d \rightarrow \mathbb{R}^d$ .

*Proof.* In order to prove this, we combine two tricks. The first is to use the adjoint stochastic differential equation, studied in Bayer and Schoenmakers [2013], to write the expectations as integrals over the transition densities  $p(t, x; T, y)$ . The second, as proposed in Heng et al. [2022], uses the Chapman-Kolmogorov equation to split the integration into smaller, approximable parts. A full proof is given in Appendix A.1.1.  $\square$

We have shown that finding  $s$  that minimises the loss function in Equation (14), also minimises Kullback-Leibler divergence between the conditioned path probability space (which we would like to access) and the path space  $\mathbb{Q}^s$ . The difference is that it is possible to approximate  $\mathcal{L}(s)$ . For example, we can take  $\epsilon$  small, and for  $t' - t$  small we can approximate  $\nabla_x \log p(t, x; t', x')$ .

## 4.2 Optimising the loss function

To solve the optimisation problem, we let  $s$  be parameterised by a neural network. We simulate batches of trajectories of the adjoint process  $\{Y(t), \mathcal{Y}(t)\}$  using the Euler-Maruyama algorithm. We then approximate the loss function as

$$\mathcal{L}(s_\theta) \approx \frac{1}{N} \sum_{Y \in B_N} \sum_{\ell=0}^{L-1} \|s_\theta(t_\ell, Y_\ell) - g(t_\ell, Y_\ell; t_{\ell+1}, Y_{\ell+1})\|^2 \mathcal{Y}(T) K(Y(T), x_0) \Delta t, \quad (15)$$

where  $Y_\ell := Y(T - t_\ell)$  and  $B_N$  is a batch of  $N$  simulations of the SDE  $Y(t)$  started at the value  $y$  on which we are conditioning. We take  $g$  to be an Euler-Maruyama step

$$g(t, x, t', x') = \frac{1}{\Delta t} (\sigma \sigma^\top)^{-1}(t, x) (x' - x - \Delta t f(t, x)), \quad (16)$$

approximating the score term  $\nabla_x \log p(t, x, t', x')$  as proposed in Heng et al. [2022]. In practice, we take  $K \equiv 1$ , which is equivalent to allowing the forward conditioned process to start from anywhere. Note that the learnt quantity  $\nabla_x \log p(t, x; T, y)$  is not dependent on  $x_0$ . The exact algorithm as described above is shown in Algorithm 1.

---

**Algorithm 1:** SDE Bridge: Condition an SDE on a fixed endpoint  $y$

---

**input:** Number of batches  $N$ , endpoint  $y$ , time grid  $\{t_\ell\}_{\ell=1}^L$   
 $\hat{t}_\ell \leftarrow T - t_{L-\ell}$   
**while** *not converged* **do**  
    For given  $y$ , compute  $N$  trajectories  $\{Y^y(\hat{t}_\ell), \mathcal{Y}^y(\hat{t}_L)\}_{\ell=1}^L$   
     $Z_\ell^y \leftarrow Y^y(\hat{t}_{L-\ell})$   
     $\mathcal{L}_\theta \leftarrow \frac{1}{(\Delta t)N} \sum_{\ell=0}^{L-1} \sum_{Z_\ell^y} \| [s_\theta(t_\ell, Z_\ell^y) - g(t_\ell, Z_\ell^y, t_{\ell+1}, Z_{\ell+1}^y)] \cdot \mathcal{Y}^y(\hat{t}_L) \|^2$   
    Compute  $\frac{d\mathcal{L}_\theta}{d\theta}$  and use it to update  $s_\theta$   
**end**

---

## 4.3 Training on multiple end points

We can extend to training on multiple end points in two ways. The first is where the end point  $y$  is not fixed, rather sampled from some distribution  $\pi_T$ . The second, is where we learn fixed  $y$  for multiple  $y$  values at once; that is for fixed  $T$  and *variable*  $y$ , we learn  $\nabla_x \log p(t, x; T, y)$ . Both of these are straightforward extensions to our method.

**Distributions of endpoints** To condition on a distribution  $\pi_T$  instead of a fixed endpoint  $y$ , we instead integrate over the loss function for different values of  $y$ . In practice, all that changes is instead of simulating trajectories  $Y, \mathcal{Y}$  starting from the same value  $y$ , we now also sample the start value  $y \sim \pi_T$ . Letting  $Y_{y,\ell} := Y_y(T - t_\ell)$ , the loss in Equation (15) function becomes

$$\mathcal{L}(s_\theta) = \frac{1}{N} \sum_{y \sim \pi_T} \sum_{\ell=0}^{L-1} \|s_\theta(t_\ell, Y_{y,\ell}) - g(t_\ell, Y_{y,\ell}; t_{\ell+1}, Y_{y,\ell+1})\|^2 \mathcal{Y}_y(T) K(Y_y(T), x_0) \Delta t. \quad (17)$$

**Multiple fixed endpoints** For varied  $y$ , we integrate the loss function in Equation (14) over  $y$  and take the loss over functions  $s: [0, T] \times \mathbb{R}^d \times \mathbb{R}^d \rightarrow \mathbb{R}^d$ . Then for the set of  $y$ 's that we are interested in, we take a batch  $B_N$  of  $N$  uniformly distributed  $y$ . In practice, the loss function that we optimise changes from Equation (15) to

$$\mathcal{L}(s_\theta) \approx \frac{1}{N} \sum_{y \in B_N} \sum_{\ell=0}^{L-1} \|s_\theta(t_\ell, Y_{y,\ell}, y) - g(t_\ell, Y_{y,\ell}; t_{\ell+1}, Y_{y,\ell+1})\|^2 \mathcal{Y}_y(T) K(Y_y(T), x_0) \Delta t. \quad (18)$$

where we have used  $Y_{y,\ell} := Y_y(T - t_\ell)$ , to mean the adjoint process  $Y$  started from  $y$  at time 0.

## 5 Experiments

In general, we compare only to methods that consider the problem where we are *given* a path distribution that we condition on given boundary conditions. This is different to the setup of generative modelling or denoising diffusion bridge models, where the boundary points or boundary distributions are given and a bridge is found between them, since in the generative modelling setup, any path distribution can be used for bridging. In this case, a natural choice is then a linear path, where transition densities  $p(t_0, x_0; t_1, x_1)$  are known explicitly.

### 5.1 Ornstein–Uhlenbeck

As a first set of experiments, we consider an Ornstein-Uhlenbeck process. For this process, the score is known and therefore we can compare exactly between the learnt and true score.

To evaluate our method, we compare to Heng et al. [2022], since they also learn the score term  $\nabla_x \log p(t, x; T, y)$ . We also compare to their learning of the term  $\nabla_{x_0} \log p(0, x_0; t, x)$ , which is used for the time-reversed bridges and must be learnt as a first step in computing the forward bridges.

In the experiments, we take the Ornstein-Uhlenbeck process defined as

$$dX(t) = -X(t)dt + dW(t). \quad (19)$$

Then the adjoint and correction processes are given by

$$dY(t) = Y(t)dt + dW(t) \quad Y(0) = y \quad (20a)$$

$$d\mathcal{Y}(t) = \mathcal{Y}(t)dt \quad \mathcal{Y}(0) = 1, \quad (20b)$$

and the score function for  $X$  is given by

$$\nabla_x \log p(t, x, s, y) = \frac{\exp\{-(s-t)\}}{v(s-t)} (y - m(s-t, x)), \quad (21)$$

where the functions  $m, v$  are the mean and variance defined as

$$m(t, x) = x \exp(-t) \quad v(t) = \frac{1 - \exp(-2t)}{2}. \quad (22)$$

In our first experiment we train on fixed end points of  $y$  that fall between  $-1.0$  and  $1.0$ , as discussed in Section 4.3. The starting values  $y$  are sampled uniformly from  $[-1, 1]$  and we train on 1000 iterations each with 1000 sample paths. We plot the absolute error of the score in Figure 1. We see the absolute error is reasonably low with slightly higher errors towards  $(-1, 1)$  and  $(1, -1)$  where the score has relatively higher values.

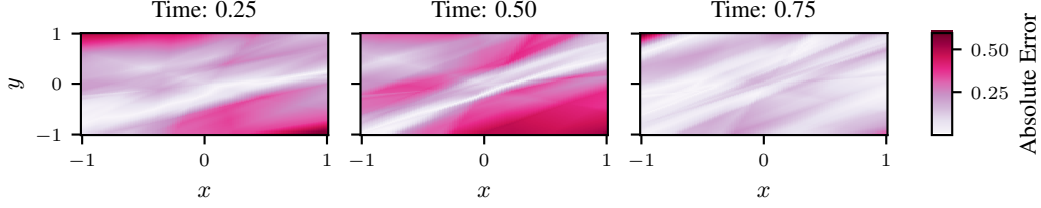


Figure 1: Trained on 1000 iterations of 1000 SDEs;  $y$  was uniformly sampled between  $-1$  and  $1$ .

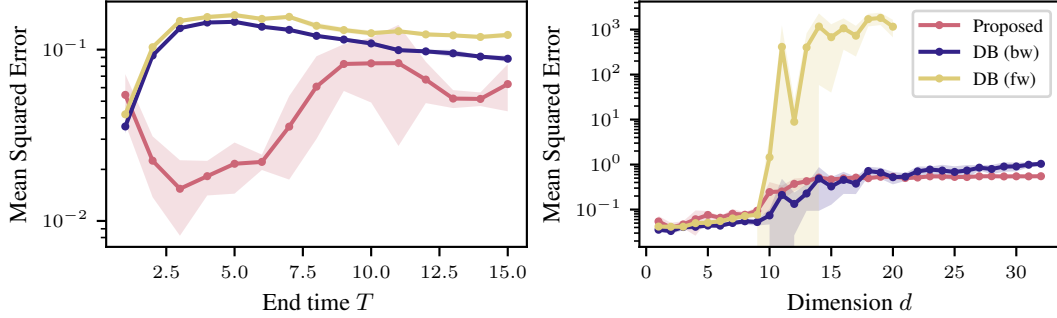


Figure 2: *Left:* Trained for  $x_0 = 1.0$ ,  $y = 1.0$ , with  $T = 1.0$ . We plot the square error between the true score and the learned score averaged over time points from  $t = 0$  to  $t = 1$ . *Right:* Trained for  $x_0 = 1$ ,  $y = 1$ , with 1-dimension and varying end times. For the proposed method and Diffusion Bridge (forward) this learns  $\nabla_x \log(t, x; T, y)$ , and for Diffusion Bridge (backward) this learns  $\nabla_x \log(0, x_0; t, x)$ . The squared errors are averaged over the time points.

To compare to the method of Heng et al. [2022], we use the code from the authors<sup>1</sup>. In Figure 2, we plot the squared error averaged over time points from  $t = 0$  to  $t = 1$  for various dimensions  $d$  with  $x_0 = 1.0$ , and various starting values  $x_0$ , with  $d = 1$ . We compare this to the forward and time-reversed (or backwards) diffusion bridges from Heng et al. [2022]. The time-reversed, DB (bw), learns a different term to ours,  $\nabla_x \log_x p(t, x; T, y)$ , and the forward, DB (fw) uses the time-reversed to learn the same term as our proposed method. For all methods we train on 100 iterations of 1000 samples. We train each one with five different random seeds and plot the average mean square error and the standard deviation between the different trainings.

We see that the Diffusion Bridge (forward) method has a similar error to the proposed method, whereas the reverse method has a much higher error and seems to break down for larger dimensions.

## 5.2 Brownian motion on distributed endpoints

To demonstrate the method in conditioning on a distribution, we next condition a Brownian motion on hitting a circle. That is, we take the SDE  $dX(t) = dW(t)$ , and we sample the end points  $y_0$  uniformly from a circle of radius 3.0. In Figure 3 (left), we plot 20 trajectories each starting from the origin, and conditioned to hit the circle at time  $T = 1.0$ . In Figure 3 (right) we plot 20 trajectories, this time starting from evenly sampled initial values on a circle of radius 5.0. Note that both figures use the same trained score function. We only need to train once, since the training is independent of the initial value  $x_0$ , and only depends on the final value or distribution that we are conditioning on.

<sup>1</sup>Via <https://github.com/jeremyhengjm/DiffusionBridge>.



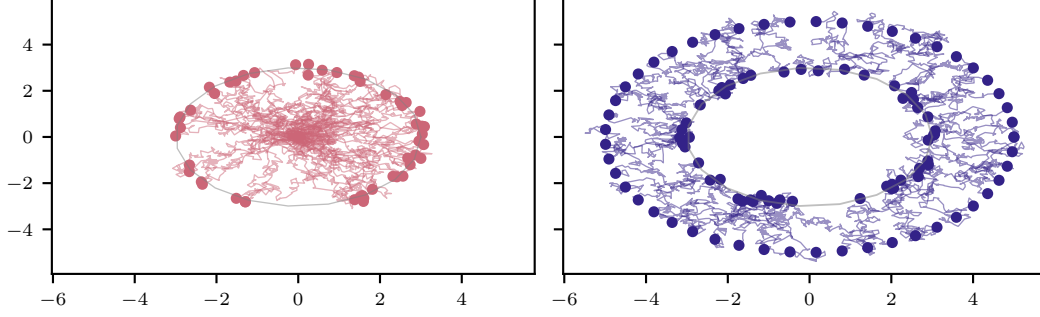


Figure 3: We train a 2 dimensional Brownian motion process to hit a circle of radius 3 at time  $T = 1.0$ . On the left we plot 20 trajectories started from the centre, and on the right we plot 20 trajectories started from evenly spaced points on a circle of radius 5.

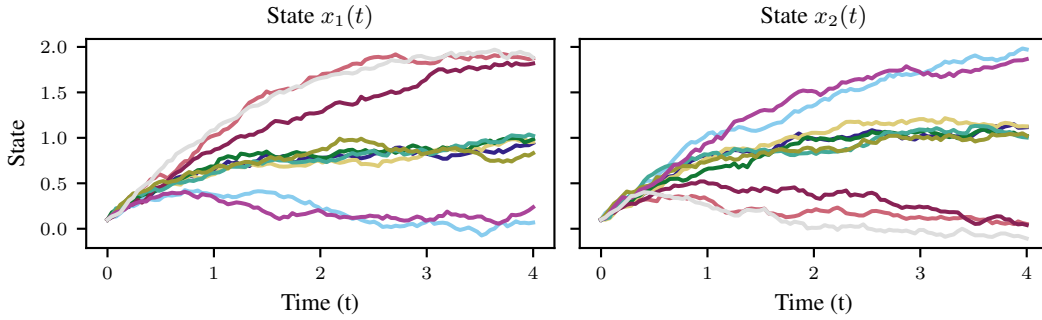


Figure 4: Trajectories from the unconditioned process of cell differentiation into three different states.

### 5.3 Cell model

We next consider the cell differentiation and development model from Wang et al. [2011]. This model is also considered in Heng et al. [2022]. The stochastic differential equation is given by

$$dx_1(t) = \frac{x_1(t)^4}{2^{-4} + x_1^4(t)} + \frac{2^{-4}}{2^{-4} + x_2^4(t)} - x_1(t)dt + \sigma dW(t) \quad (23)$$

$$dx_2(t) = \frac{x_2(t)^4}{2^{-4} + x_2^4(t)} + \frac{2^{-4}}{2^{-4} + x_1^4(t)} - x_2(t)dt + \sigma dW(t), \quad (24)$$

and describes the process of cell differentiation into three specific cell types. In Figure 4 we plot some trajectories for the unconditioned process for illustration purposes. In our experiment we compare to the time-reversed bridge and the forward bridge of Heng et al. [2022] (again using the code from the authors <sup>2</sup>) and the guided bridge method from Schauer et al. [2017]. The true bridge is unknown, so instead we compare against trajectories from the unconditioned process that end near the boundary values. In Figure 5, we plot in grey trajectories from the unconditioned process satisfying  $1.3 < x_1(T) < 1.7, 0.0 < x_2(T) < 0.4$  at time  $T = 2.0$ . We then plot trajectories starting at  $(0.1, 0.1)$ , conditioned on  $(1.5, 0.2)$  at time  $T = 2.0$ , via the proposed method, the forward bridge (DB) of Heng et al. [2022] and with MCMC using guided proposals as suggested in Schauer et al. [2017].

For the time-reversed bridge, the trajectories are simulated starting at the end point  $(1.5, 2.0)$ , and run backwards in time, being conditioned to hit the point  $(0.1, 0.1)$ . We then use trajectories from the time-reversed SDE to train the forward bridge as stated in Heng et al. [2022, Section 2.3]. For the proposed method, the time-reversed bridge (DB) and the forward bridge (DB), we train on 10,000

<sup>2</sup><https://github.com/jeremyhengjm/DiffusionBridge>

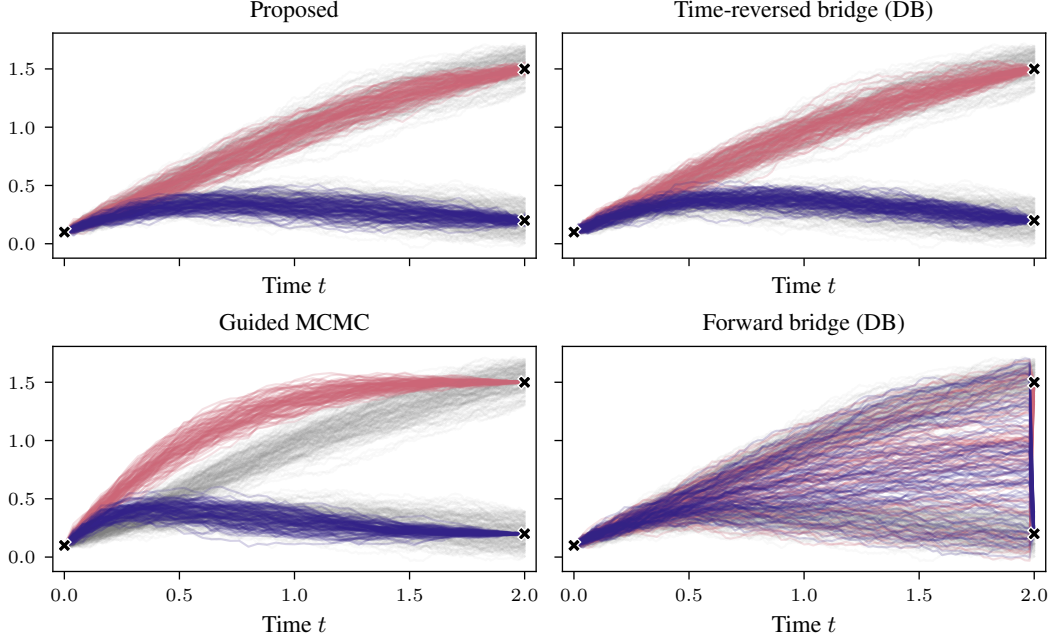


Figure 5: We plot 100 trajectories. *Proposed*, *Guided MCMC* and *Forward bridge (DB)* are started from the point  $(0.1, 0.1)$  and are conditioned on  $(1.5, 0.2)$  at time  $t = 2$ . *Time-reversed bridge* is started from  $(1.5, 0.2)$  at time  $t = 2$  and conditioned on hitting  $(0.1, 0.1)$  at time  $t = 0$ . In grey, we plot some unconditioned trajectories that end in a given window about the point  $(1.5, 0.2)$ .

trajectories in total with batch sizes of 100. We use the same network structure for both the proposed method and the time-reversal with the same number of layers, however the proposed method is written in Jax [Bradbury et al., 2018], whereas the other uses Pytorch [Paszke et al., 2019].

For the guided method we use the code from the authors<sup>3</sup>. We first simulate 1000 trajectories, without saving, and from then save every 100<sup>th</sup> trajectory, with  $\rho = 0.7$ .

We see in Figure 5 that the proposed method and the time-reversed bridge both produce similar trajectories that seem to follow the correct data distribution. However, the forward in time bridge seems to break down entirely.

## 6 Advantages, disadvantages and concluding remarks

We have shown that we can use adjoint processes to learn the score term  $\nabla \log p(t, X; T, y)$  for given  $T, y$ . This is applied to simulate forward trajectories of bridged diffusion processes. When compared to the method in Heng et al. [2022] for simulating forward in time bridges, we have demonstrated in our experiments that using the adjoints leads to a more stable estimation with lower error. Learning the score also seems to perform well when compared to using MCMC methods to sample trajectories. However, we note that MCMC methods will likely perform better when conditioning on extremely unlikely events, that will not be seen in the generated data.

<sup>3</sup>Codebase at <https://github.com/mschauer/Bridge.jl> from file `project/partialbridge_fitzhugh.jl`

## 7 Acknowledgements

The work presented in this article was done at the Center for Computational Evolutionary Morphometry and is partially supported by the Novo Nordisk Foundation grant NNF18OC0052000, by the Chalmers AI Research Centre (CHAIR) (“Stochastic Continuous-Depth Neural Network”) as well as a research grant (VIL40582) from VILLUM FONDEN and UCPH Data+ Strategy 2023 funds for interdisciplinary research.

## References

- Bernard Delyon and Ying Hu. Simulation of conditioned diffusion and application to parameter estimation. *Stochastic Processes and their Applications*, 116(11):1660–1675, November 2006. ISSN 03044149.
- Omiros Papaspiliopoulos and Gareth Roberts. Importance sampling techniques for estimation of diffusion models. *Statistical methods for stochastic differential equations*, 124:311–340, 2012.
- Mogens Bladt and Michael Sørensen. Simple simulation of diffusion bridges with application to likelihood inference for diffusions. *Bernoulli*, pages 645–675, 2014.
- Moritz Schauer, Frank Van Der Meulen, and Harry Van Zanten. Guided proposals for simulating multi-dimensional diffusion bridges. *Bernoulli*, 23(4A), November 2017. ISSN 1350-7265. doi: 10.3150/16-BEJ833.
- Jeremy Heng, Valentin De Bortoli, Arnaud Doucet, and James Thornton. Simulating diffusion bridges with score matching, October 2022. arXiv:2111.07243.
- Raghav Singhal, Mark Goldstein, and Rajesh Ranganath. What’s the score? Automated denoising score matching for nonlinear diffusions. In *Forty-first International Conference on Machine Learning*, 2024.
- Alexis Arnaudon, Darryl D Holm, Akshay Pai, and Stefan Sommer. A stochastic large deformation model for computational anatomy. In *Information Processing in Medical Imaging: 25th International Conference, IPMI 2017, Boone, NC, USA, June 25-30, 2017, Proceedings 25*, pages 571–582. Springer, 2017.
- Elizabeth Louise Baker, Gefan Yang, Michael L. Severinsen, Christy Anna Hipsley, and Stefan Sommer. Conditioning non-linear and infinite-dimensional diffusion processes, February 2024. arXiv:2402.01434.
- Grigori N. Milstein, John G.M. Schoenmakers, and Vladimir Spokoiny. Transition density estimation for stochastic differential equations via forward-reverse representations. *Bernoulli*, 10(2), April 2004. ISSN 1350-7265. doi: 10.3150/bj/1082380220.
- René L. Schilling and Lothar Partzsch. *Brownian motion: an introduction to stochastic processes*. De Gruyter textbook. de Gruyter, Berlin ; Boston, second edition edition, 2014. ISBN 978-3-11-030729-0.
- Simo Särkkä and Arno Solin. *Applied Stochastic Differential Equations*. Cambridge University Press, 1 edition, April 2019. ISBN 978-1-108-18673-5 978-1-316-51008-7 978-1-316-64946-6. doi: 10.1017/9781108186735.
- Ulrich G Haussmann and Etienne Pardoux. Time reversal of diffusions. *The Annals of Probability*, pages 1188–1205, 1986.
- Christian Bayer and John Schoenmakers. Simulation of forward-reverse stochastic representation for conditional diffusions. *The Annals of Applied Probability*, 24, June 2013. doi: 10.1214/13-AAP969.

- Frank Van der Meulen and Moritz Schauer. Automatic backward filtering forward guiding for Markov processes and graphical models, 2020. 2010.03509v2.
- Aapo Hyvärinen. Estimation of non-normalized statistical models by score matching. *Journal of Machine Learning Research*, 6(24):695–709, 2005.
- Pascal Vincent. A connection between score matching and denoising autoencoders. *Neural computation*, 23(7):1661–1674, 2011.
- Jonathan Ho, Ajay Jain, and Pieter Abbeel. Denoising diffusion probabilistic models. *Advances in neural information processing systems*, 33:6840–6851, 2020.
- Asger Roer Pedersen. Consistency and asymptotic normality of an approximate maximum likelihood estimator for discretely observed diffusion processes. *Bernoulli*, pages 257–279, 1995.
- Jin Wang, Kun Zhang, Li Xu, and Erkang Wang. Quantifying the Waddington landscape and biological paths for development and differentiation. *Proceedings of the National Academy of Sciences*, 108(20):8257–8262, 2011.
- James Bradbury, Roy Frostig, Peter Hawkins, Matthew James Johnson, Chris Leary, Dougal Maclaurin, George Necula, Adam Paszke, Jake VanderPlas, Skye Wanderman-Milne, and Qiao Zhang. JAX: composable transformations of Python+NumPy programs, 2018. URL <http://github.com/google/jax>.
- Adam Paszke, Sam Gross, Francisco Massa, Adam Lerer, James Bradbury, Gregory Chanan, Trevor Killeen, Zeming Lin, Natalia Gimelshein, Luca Antiga, et al. Pytorch: An imperative style, high-performance deep learning library. *Advances in neural information processing systems*, 32, 2019.

## A Appendix

### A.1 Proofs

#### A.1.1 Proof of Theorem 4.1

**Theorem.** Let  $\mathbb{P}^y$  be the path probability of the conditioned diffusion  $X^y$  in Equation (2), and  $\mathbb{Q}^s$  the path probability of  $X^s$  in Equation (13) for a function  $s$ . Then

$$\inf_s \text{KL}(\mathbb{P}^y \parallel \mathbb{Q}^s) = \inf_s \mathcal{L}(s),$$

where the infimum is taken over functions  $s: [0, T] \times \mathbb{R}^d \rightarrow \mathbb{R}^d$ .

*Proof.* The Kullback-Leibler divergence is defined by

$$\text{KL}(\mathbb{P}_y \parallel \mathbb{Q}_\theta) = \int \log \frac{d\mathbb{P}_y}{d\mathbb{Q}_\theta} d\mathbb{P}_y(X). \quad (25)$$

By Girsanov’s theorem, [Schilling and Partzsch, 2014, Theorem 19.9]

$$\frac{d\mathbb{P}_y}{d\mathbb{Q}_\theta}(X) = \exp \left( -\frac{1}{2} \int_0^T \|\sigma^\top(s - s_\theta)(t, X_t)\|^2 dt + \int_0^T \sigma^\top(s - s_\theta)(t, X_t) dB_t \right). \quad (26)$$

Since the expectation of a martingale is equal to 0, we see that

$$\text{KL}(\mathbb{P}_y \parallel \mathbb{Q}_\theta) = \int_{X \in \mathcal{X}} \left[ -\frac{1}{2} \int_0^T \|(s - s_\theta)(t, X_t)\|_{\sigma\sigma^\top}^2 dt \right] d\mathbb{P}_y(X) \quad (27a)$$

$$= -\frac{1}{2} \int_0^T \mathbb{E}^y \left[ \|(s - s_\theta)(t, X_t)\|_{\sigma\sigma^\top}^2 \right] dt \quad (27b)$$

$$= -\frac{1}{2} \int_0^T \mathbb{E} \left[ \|(s - s_\theta)(t, X_t)\|_{\sigma\sigma^\top}^2 \mid X_{0,x_0}(T) = y \right] dt. \quad (27c)$$

By [Bayer and Schoenmakers, 2013, Theorem 3.7], this is equal to

$$-\frac{1}{2p(0, x_0; T, y)} \int_0^T \lim_{\epsilon \rightarrow 0} \mathbb{E} [\|(s - s_\theta)(t, Y(T-t))\|_{\sigma\sigma^\top}^2 \mathcal{Y}(T) K_\epsilon(Y(T), x_0)] dt. \quad (28)$$

We next focus on the contents of the expectation. Writing  $s$  out in full as  $s = \nabla_x \log p(t, x; T, y)$ , using  $K_\epsilon$  in place of  $K_\epsilon(Y(T), x_0)$  and expanding the square, we see

$$\int_0^T \mathbb{E} [\|(s - s_\theta)(t, Y(T-t))\|_{\sigma\sigma^\top}^2 \mathcal{Y}(T) K_\epsilon(Y(T), x_0)] dt \quad (29a)$$

$$= \mathbb{E} \left[ \int_0^T \|s_\theta(t, Y(T-t))\|^2 \mathcal{Y}(T) K_\epsilon dt \right] \quad (29b)$$

$$+ \mathbb{E} \left[ \int_0^T \|\nabla \log p(t, Y(T-t); T, y)\|^2 \mathcal{Y}(T) K_\epsilon dt \right] \quad (29c)$$

$$- 2\mathbb{E} \left[ \sum_{\ell=1}^L \int_{t_{\ell-1}}^{t_\ell} s_\theta(t, Y(T-t)) \cdot \nabla \log p(t, Y(T-t); T, y) \cdot \mathcal{Y}(T) K_\epsilon dt \right]. \quad (29d)$$

We focus on the third term, Equation (29d). Multiplying this out further and using [Bayer and Schoenmakers, 2013, Theorem 3.6], we see that

$$\mathbb{E} [s_\theta(t, Y(T-t)) \cdot \nabla \log p(t, Y(T-t); T, y) \cdot \mathcal{Y}(T)] \quad (30a)$$

$$= \int s_\theta(t, x) \nabla_x \log p(t, x, T, y) p(t_0, x_0; t, x) p(t, x; T, y) dx_0 dx \quad (30b)$$

$$= \int s_\theta(t, x) \nabla_x p(t, x; T, y) p(t_0, x_0; t, x) dx_0 dx. \quad (30c)$$

Using Chapman-Kolmogorov it holds that for any  $t < t_1 < T$ ,

$$p(t, x; T, y) = \int p(t, x; t_1, x_1) p(t_1, x_1; T, y) dx_1, \quad (31)$$

and so, using the properties of the differential of the logarithm it holds

$$\nabla_x p(t, x; T, y) = \int \nabla_x \log p(t, x; t_1, x_1) p(t, x; t_1, x_1) p(t_1, x_1; T, y) dx_1. \quad (32)$$

Putting this back into Equation (30c) and using Bayer and Schoenmakers [2013, Theorem 3.6] we get,

$$\int [s_\theta(t, x) \nabla_x \log p(t, x; t_1, x_1)] p(t_0, x_0; t, x) p(t, x; t_1, x_1) p(t_1, x_1; T, y) dx_0 dx dx_1 \quad (33a)$$

$$= \mathbb{E} [s_\theta(t, Y(T-t)) \nabla \log p(t, Y(T-t); t_1, Y(T-t_1)) \mathcal{Y}(T)]. \quad (33b)$$

From this we see that Equation (29d) becomes

$$-2\mathbb{E} \left[ \sum_{\ell=1}^L \int_{t_{\ell-1}}^{t_\ell} s_\theta(t, Y(\hat{t})) \nabla \log p(t, Y(\hat{t}); t_\ell, Y(\hat{t}_\ell)) \mathcal{Y}(T) K_\epsilon dt \right]. \quad (34)$$

Then Equation (29a) is equal to

$$\sum_{\ell=1}^L \int_{t_{\ell-1}}^{t_{\ell}} \mathbb{E} [\|s_{\theta}(t, Y(\hat{t})) - \nabla \log p(t, Y(\hat{t}); t_{\ell}, Y(\hat{t}_{\ell}))\|^2 \mathcal{Y}(T) K_{\epsilon}] dt + \text{const.}, \quad (35)$$

where

$$\text{const.} = \sum_{\ell=1}^L \int_{t_{\ell-1}}^{t_{\ell}} [\|\nabla \log p(t, Y(\hat{t}); T, y)\|^2 - \|\nabla \log p(t, Y(\hat{t}); t_{\ell}, Y(\hat{t}_{\ell}))\|^2] \mathcal{Y}(T) K_{\epsilon} dt. \quad (36)$$

□